HHS Public Access

Author manuscript

Nitric Oxide. Author manuscript; available in PMC 2019 September 01.

Published in final edited form as:

Nitric Oxide. 2018 September 01; 79: 57–67. doi:10.1016/j.niox.2018.07.005.

Detection of Dinitrosyl Iron Complexes by Ozone-based Chemiluminescence

George T. Mukosera[1], **Taiming Liu**[1], **Abu Shufian Ishtiaq Ahmed**[3,5], **Qian Li**[4], **Matilda H.-C. Sheng**[3], **Trent E. Tipple**[4], **David J. Baylink**[3], **Gordon G. Power**[2], and **Arlin B. Blood**[1,2]

[1]Department of Pediatrics, Loma Linda University School of Medicine, Loma Linda, CA, 92354, USA

[2]Lawrence D. Longo Center for Perinatal Biology, Loma Linda University School of Medicine, Loma Linda, CA, 92354, USA

[3]Regenerative Medicine Division, Department of Medicine, Loma Linda University School of Medicine, Loma Linda, CA 92354, USA

[4]Neonatal Redox Biology Laboratory, Department of Pediatrics, University of Alabama at Birmingham, Birmingham, AL 35294, USA

[5]Center for Dental Research, Loma Linda University School of Dentistry, Loma Linda, CA, 92350, USA

Abstract

Dinitrosyl iron complexes (DNICs) are important intermediates in the metabolism of nitric oxide (NO).They have been considered to be NO storage adducts able to release NO, scavengers of excess NO during inflammatory hypotensive shock, and mediators of apoptosis in cancer cells, among many other functions. Currently, all studies of DNICs in biological matrices use electron paramagnetic resonance (EPR) for both detection and quantification. EPR is limited, however, by its ability to detect only paramagnetic mononuclear DNICs even though EPR-silent binuclear are likely to be prevalent. Furthermore, physiological concentrations of mononuclear DNICs are usually lower than the EPR detection limit (1 μM). We have thus developed a chemiluminescence-based method for the selective detection of both DNIC forms at physiological, pathophysiological, and pharmacologic conditions. We have also demonstrated the use of the new method in detecting DNIC formation in the presence of nitrite and nitrosothiols within biological fluids and tissue. This new method, which can be used alone or in tandem with EPR, has the potential to offer insight about the involvement of DNICs in many NO-dependent pathways.

Correspondence to: Arlin B. Blood.

* Corresponding author: abblood@llu.edu.

Keywords

Dinitrosyl iron complexes (DNICs); nitric oxide; glutathione; nitric oxide stores; chemiluminescence; EPR

1. Introduction

Nitric oxide (NO) is a diverse and nearly ubiquitous biological signaling molecule. Although it is produced primarily from L-arginine by NO synthase (NOS) enzymes, significant versatility in NO signaling is derived from the ability of many of its metabolites to either be converted back into NO or to participate in their own unique signaling pathways. Ozone-based chemiluminescent detection of NO has been a mainstay in the study of these metabolites. The method, which detects NO in gaseous form, can be applied by injecting samples into a vessel purged with an inert gas that carries freed NO into the analyzer. Further refinement of the method has resulted in the use of various chemical reagents in the purge vessel that facilitate the selective release of NO from specific classes of NO metabolites, including nitrite [1], nitrosothiols [2], and heme nitrosyls [3].

Dinitrosyl iron complexes (DNICs) are a class of NO metabolites that has received relatively little attention in the validation of chemiluminescence-based assays. DNICs are comprised of an iron metal center which is bound to two nitric oxide (NO) moieties, and commonly two additional thiolate or amino ligands in biological systems [4]. DNICs exist in two forms – a mononuclear (one iron atom) form (MDNIC), which is paramagnetic and thus detectable by electron paramagnetic resonance (EPR), and a binuclear form (BDNIC), which is diamagnetic and thus EPR-silent [5]. Depending on their ligands, DNICs can be very stable storage forms of NO, with higher molecular weight ligands being the most stable and least likely to release NO through spontaneous decay [6, 7]. This ligand-dependent stability is thought to make DNICs tunable for the storage, transport and release of NO under varying physiological conditions. For instance, high molecular weight DNIC formation has been reported in smooth muscle cells, endothelial cells, macrophages and tumor cells after exposure to lipopolysaccharide, inflammatory cytokines, or NO donors, and are proposed to sequester excess NO resulting in protection from NO-cytotoxicity [8–10]. Low molecular weight glutathione-liganded DNICs (glut-DNIC) have been reported to be a transport form of iron through a multi-drug resistance associated protein transporter during NO-mediated iron efflux from tumor cells [11, 12]. In the presence of even lower molecular weight L-cysteine or N-acetylcysteine ligands, DNICs have been observed to act more like a traditional NO-donor, resulting in NO-related effects such as rapid vasorelaxation of pre-contracted smooth muscle cells [13]. DNICs may also prove to have therapeutic importance since glut-DNIC is currently in Phase II clinical trials as a stable NO-donor for the treatment of hypertension [14].

Despite their emerging importance, the detection and quantification of DNICs has been limited solely to EPR. This methodology is often inadequate, however, as it only detects MDNICs. Furthermore, the lower limit of detection and quantification of MDNICs by EPR is ~1 μM (with respect to the iron, 2 μM with respect to NO), which is above both bioactive

and physiological levels [15]. Consequently, relatively little is known about the prevalence and role of DNICs under physiological conditions. To address the lack of tools available to characterize and quantify DNICs, we have adapted ozone-based chemiluminescence to selectively detect both M- and BDNICs in biological matrices in the presence of two other prevalent co-existing NO metabolites and synthesis-contaminants, nitrite and nitrosothiols.

Considering the limitations of EPR for measuring DNICs, the chemiluminescence-based method we describe affords itself as a promising alternative. The method can be used for the selective detection of DNICs under physiological, pathophysiological and pharmacological conditions. Through our consideration of the main metabolites of DNICs, we have simultaneously validated chemiluminescence-based methods that can be used to selectively discriminate nitrite and nitrosothiols from each other, and from B/MDNICs without the need of pretreating samples with chemical additives, which is the standard practice in NOx detection by chemiluminescence.

2. Materials and Methods

All chemicals for DNIC synthesis and for use in purge vessels were obtained from Sigma (St. Louis, MO). 1-(hydroxy-NNO-azoxy)-L-proline, disodium salt (ProliNONOate) was obtained from Cayman Chemicals (Ann Harbor, MI). 17.4 N Glacial acetic acid was obtained from Fisher Scientific (Pittsburgh, PA). Lipopolysaccharide (LPS) was obtained from Sigma (St. Louis, MO) for use in the studies of rats and cell culture.

Sheep plasma was obtained by venipuncture of the jugular vein of unanesthetized adult ewes to collect blood. The blood was collected in heparinized syringes, and centrifuged at 2,500 rpm for 15 minutes within 30 minutes of blood collection.

2.1. Preparation of GSNO, MDNIC, and BDNIC

S-nitrosoglutathione (GSNO) was prepared by mixing equimolar amounts of glutathione and nitrite acidified with 1 M HCl, reacting over ice for two hours, and storing aliquots at −80 °C. The yield in GSNO was at least 95% across multiple syntheses, and no appreciable changes in GSNO stock solution concentrations were detected in the aliquots stored at −80 °C for more than 12-months. GSNO dilutions were always made in PBS buffer at pH = 7.4 with 0.1 mM diethylenetriamine-pentaacetic acid (DTPA) added as a metal chelator. Aliquots from the same batch of GSNO were used throughout the study.

Mononuclear dinitrosyl iron complex and binuclear dinitrosyl iron complexes with glutathione ligands, glut-MDNIC and glut-BDNIC respectively, were prepared as described by Vanin and coworkers [16]. In brief, glut-BDNIC was prepared by mixing two equivalents of glutathione with one equivalent of resulting GSNO was subsequently incorporated into glut-BDNIC by adjusting the pH with drop-wise addition of 1M NaOH to neutralize the pH. After an overnight incubation at room temperature in the dark, the precipitated iron hydroxides were removed via centrifugation and decanting. Part of the supernatant was separated into aliquots and stored at −80 °C. glut-MDNIC was subsequently obtained from the remaining supernatant by adding another equivalent of glutathione, adjusting the pH to 10.0 with 1 M NaOH, and incubating for three to four hours at room temperature in the dark.

glut-MDNIC aliquots were also stored at −80 °C. The same batches of glut-MDNIC and glut-BDNIC were used throughout the study.

2.2. Spectrophotometric characterization

Optical properties of GSNO, glut-MDNIC and glut-BDNIC were obtained using a Thermo Scientific® NanoDrop 2000 UV-Vis spectrophotometer with a 10-mm optical path length. Extinction coefficients used for glut-BDNIC and glut-MDNIC concentration calculations were as provided by Vanin and coworkers: 9200 and 7400 $M^{-1}cm^{-1}$ for the glut-BDNIC characteristic peaks at 310 and 360 nm respectively, and 4700 $M^{-1}cm^{-1}$ for the glut-MDNIC characteristic peak at 390 nm [16]. An extinction coefficient of 922 $M^{-1}cm^{-1}$ at 335 nm was used for GSNO [17].

2.3. EPR characterization

EPR spectra of glut-MDNIC preparations were measured using a modified Radiopan EPR spectrophotometer (Poland) (microwave power 5 mW, modulation amplitudes 0.05–2 mT) at ambient temperature or at 77 K. The glut-MDNIC concentrations were determined by double integration of the EPR signals. Iron-nitrosyl myoglobin (MbNO) solutions of known concentrations in PBS with 100 μM DPTA were used to create a calibration curve, which was used to calculate glut-MDNIC concentrations [18].

2.4. Ozone-based chemiluminescence

Nitric oxide was measured by a gas phase chemiluminescence reaction of NO with ozone using a Nitric Oxide Analyzer (NOA) (Sievers NOA 280i, Boulder, CO). In each of the different assays to be described DNICs, nitrite and nitrosothiols react so as to release NO in the purge vessel of the analyzer using appropriate reagents. The released NO gas is carried by a stream of inert gas (argon) to the detector where it reacts with ozone to produce a chemiluminescence signal proportional to the concentration.

The NO-release peak profiles of glut-DNICs, nitrite and GSNO (1000 pmol) were monitored in real time using proprietary software (Liquid version v3.21, Sievers), which was also used to report the area under the curve for each NO-release profile, and for calibration of the reagents and quantification of the NO_x species concentrations. The NO-release peaks were exported to Prism 7.0 software (Graphpad Software, Inc, La Jolla, CA) for better display.

Due to the day-to-day and across-instrument variability in the detector sensitivity, an index of which was taken to be proportional to the slope of the NO amount vs. the respective area under curve (AUC), reported AUCs were normalized to an ideal slope of 7.0 mV.hr/pmol. This allowed easier comparison of data from instruments with differing detector sensitivity.

2.5. Characterization of high molecular weight DNICs

High molecular weight DNICs were made by adding glut-BDNIC or glut-MDNIC to ovine plasma at 37 °C and incubating for five minutes, as previously described [19]. High and low molecular weight species were separated in a 2.5 mL 5000 kD size exclusion column (G25 Sephadex, GE Healthcare Life Sciences, Pittsburgh, PA), and the eluent was collected on ice with six drops per fraction.

2.6. Detection of LPS-stimulated DNICs in rat plasma and tissue

All animal protocols were approved by the Loma Linda University Institutional Animal Care and Use Committee. Lipopolysaccharide (LPS, 1 mg/100 g of rat weight) or saline as control was injected intraperitoneally into 1- to 2-month old Sprague-Dawley rats. To confirm a response to LPS, the anorectal temperature of the rats was followed hourly to detect the temperature drop that is characteristic of rats under LPS-treatment [20]. After six hours the rats were deeply anesthetized with 4% isoflurane. Following a thoracotomy, whole blood was collected via cardiac puncture into a heparinized syringe, one aliquot of which was immediately snap frozen. Another aliquot was centrifuged at 14,000 rpm for 60 seconds for collection and snap-freezing of the plasma fraction. Following perfusion of the peripheral organs with a cold solution of PBS (pH=7.4) through the left ventricle to minimize organ blood content, the liver, was excised, snap frozen in liquid nitrogen, and stored at −80 °C. At a later date, the liver tissue was thawed, placed in PBS (8 mL per 1 g of tissue), and homogenized on ice (TissueRuptor, Qiagen). After centrifuging for 10 minutes at 100 rpm to remove tissue debris, the supernatant was decanted, snap concentrations. The heme content of the supernatant was additionally assayed using a total heme assay kit (MAK316–1KT, Sigma, St. Louis, MO).

To test further for possible formation of DNICs in tissue, liver tissue homogenates were treated with make ~100 mM solution. After a 5-min incubation the tissue debris was removed using a 6-mL syringe filled with surgical gauze that had been rinsed with deionized water. The effluent from the filtered homogenates was injected without delay into the purge vessels of two simultaneously running NOA-instruments for detection of free NO gas and DNICs as described below.

2.7. Cell Culture

Murine macrophage RAW 264.7 cells were purchased from American Type Culture Collection (ATCC, Manassas, VA) and maintained in Dulbecco's modified Eagle's medium (DMEM, Gibco, Life Technologies) supplemented with 10% heat-inactivated fetal bovine serum (FBS) and 1% penicillin streptomycin (Gibco, Life Technologies) at 37 °C in a 5% CO2 atmosphere. Cells up to passage 17 were used and the medium was changed every three days.

2.8. Detection of LPS-stimulated DNICs in macrophages

The cells were seeded onto 10-cm plates with 5.5 × 106 cells per 10 mm plate and incubated for 24 hours at 37°C in a humidified atmosphere containing 5% CO2. After PBS wash, cells were treated with 1 μg/mL or 5 μg/mL of LPS for ten hours. A portion of culture media was collected for analysis. The cells were washed with PBS and finally all the cells were collected in 800 μL of PBS using a cell scraper. Cells were lysed by freeze-thaw cycles repeated three times, after which the NOx content of the cell lysates and the cell media was analyzed by chemiluminescence with different purge vessel reagents. In a variation of the experiment, cells were cultured in DMEM media that was supplemented with 100 μM FeSO4 for 24 hours to increase the intracellular chelatable iron, which has been found to aid in DNIC formation [22]. The cells were subsequently rinsed and the cell media was replaced before LPS-treatment.

2.9. Statistical Analysis

All results are expressed as mean±SEM with p-values ≤ 0.05 considered statistically significant. Student's t-tests were used to test for significant differences between NOx levels in control vs. LPS treated rat tissue or plasma for each of the selective reagent. Slopes and intercepts of calibration curves were compared using the linear regression analysis function in Graphpad Prism. All Analyses was carried out using Graphpad Prism 7.0 software (Graphpad Software, La Jolla, CA).

3. Results

Characterization of glut-DNICs by EPR and spectrophotometry

Both EPR and spectrophotometry were used to characterize the purity and concentration of the glut-DNICs that were synthesized for use as standards. The EPR spectra from the synthesized glut-MDNIC (Figure S1A) were in agreement with the literature reports [16]. As expected, glut-BDNIC did not exhibit a detectable EPR signal. However, given that glut-MDNIC is synthesized secondary to glut-BDNIC synthesis, evidence of successful production of glut-MDNIC indicates that glut-BDNIC was also produced successfully.

The optical results were also consistent with earlier literature reports, yielding the characteristic absorption maximum of 390 nm for glut-MDNIC and 310 and 360 nm for glut-BDNIC (Figure S1B). The published extinction coefficients of glut-MDNIC (4700 $M^{-1}cm^{-1}$), and glut-BDNIC (9200 and 7400 $M^{-1}cm^{-1}$) were used for DNIC quantification [16]. Our synthetic protocol produced DNICs with yields ranging from 50 to 80% of initial iron concentrations. Due to this variability in DNIC yield, all aspects of the study were performed using DNICs obtained from a single batch. There was negligible interference from GSNO (Figure S1B) or from nitrite (data not shown) at the maximum absorbance of glut-B- and glut-MDNIC.

Characterization of glut-DNICs by ozone-based chemiluminescence

For the selective detection of DNICs, nitrite, and SNOs, ozone-based chemiluminescent detection of NO was coupled with the injection of samples into a purge vessel containing reagents capable of facilitating selective release of the NO moiety from one or more of the three classes of NOx species. The purge vessel reagents, all of which were adapted from literature and then optimized in our laboratory, were triiodide in glacial acetic acid (Ac/I_3^-) [23, 24], ascorbic acid in glacial acetic acid (Ac/Asc) [25, 26], 10 μM Cu^{2+} added to ascorbic acid in glacial acetic acid (Ac/Asc/Cu^{2+}) [2], potassium ferricyanide in glacial acetic acid (Ac/FeCN) [3], and potassium ferricyanide in PBS (pH = 7.4, PBS/FeCN) [27]. The preparation of these reagents and a detailed account of their respective chemistries are described in the Supplementary information. A summary of the reagents' hypothesized specificities for NO release from iron nitrosyls, nitrite, and nitrosothiols is given in Table 1.

To assess the specificity of the reagents in Table 1, nitrite, GSNO, glut-BDNIC, or glut-MDNIC were added to either deionized water or plasma to achieve a final concentration of 10 μM with respect to NO moieties released by the triiodide reagent, and kept on ice to minimize metabolic changes. Within 30 seconds after addition of the NOx species, before

any appreciable metabolism of the DNICs by the plasma, resulting solutions were then injected into a purge vessel containing one of the reagents shown in Table 1. Overall, the selectivities of the reagents were similar between plasma and deionized water, as can be seen by comparing Figure 1 with Figure S3. An exception was the Ac/Asc/Cu^{2+} assay which had such low sensitivity in plasma samples that it was deemed not suitable for plasma measurements. However, this reagent was still useful in estimating the amount of nitrite and nitrosothiol contamination in stock solutions of DNICs, as demonstrated in the Supplementary information.

As expected, nitrite, GSNO, glut-BDNIC, and glut-MDNIC all released NO when added to a purge vessel with triiodide for both deionized water and plasma solutions (Figures 1 and S3A). The recovered NO amount, proportional to the area under the curve (AUC), was similar across the different NOx species (Figures 1B and S3B), indicating the NO released for each NOx species was quantitative. However, the rate of NO release from glut-DNICs was slower than from nitrite and GSNO, as demonstrated by the broader peak shapes of the DNICs.

We next evaluated the Ac/Asc reagent, which was expected to detect only nitrite. Ac/Asc resulted in quantitative release of NO from nitrite, with only miniscule peaks observed from GSNO and glut-DNICs (Figure 1C, D). These were eliminated by pretreatment of the samples with acidified sulfanilamide to remove nitrite. Since sulfanilamide-sensitive peaks of similar size were also found in the deionized water solutions (Figure S3), the peaks most likely arose from nitrite contamination in the GSNO and DNIC standards rather than release of NO from GSNO/DNICs *per se*. In sum, the results indicate the Ac/Asc assay is selective for nitrite and does not detect glut-DNICs, an observation that has not been noted previously. Earlier studies have shown the Ac/Asc assay does not detect nitrated lipids, nitrosamines, or RSNOs [25].

Tests of the selectivity of the Ac/FeCN reagent, expected to selectively detect nitrite and glut-DNICs but not GSNO, and of the PBS/FeCN reagent, expected to detect glut-DNICs but not nitrite or GSNO, are shown in in Figure 1E through H. Consistent with expectations (Table 1), the Ac/FeCN assay detected NO release only following injection of nitrite or glut-DNICs, with a negligible peak from GSNO that was again attributable to nitrite contamination. Notably, and similar to the observation made in triiodide, the rate of NO release from nitrite was faster than from glut-B/MDNIC as demonstrated by the difference in peak shapes. Also, consistent with prediction, the PBS/FeCN assay did not detect a signal from either nitrite or GSNO (Figure 2G, H), but did detect NO released from the glut-B/MDNICs, albeit at a slower rate than in triiodide as evidenced by the broader peaks (Figure 2G and H). Despite considerable peak broadening in the PBS/FeCN assay, detection of at least 0.1 μM (10 pmol) of low molecular weight DNIC was possible, with quantification possible at concentrations > 0.3 μM, after injection of a 100 μL sample. Pretreament of samples with acidified sulfanilamide is often assumed to selectively remove nitrite without affecting the concentrations of other NOx species [24]. However, contrary to this assumption, we observed a significant decrease in the amount of NO released from DNICs in the PBS/FeCN reagent, suggesting that a fraction of the DNICs was lost by acid sulfanilamide pretreatment (Figure 2F, H). In addition, while the amount of contaminating

nitrite detected in the Ac/Asc assay was in the range of 5 to 10% of the nominal 10 mM DNIC injection, acid sulfanilamide pretreatment resulted in ~50% decreases in the amount of NO released from DNICs in the Ac/FeCN reagent, again suggesting that the DNICs may not be stable in the presence of acidified sulfanilamide treatment.

Qualitative assessments of peak shapes

Although the amounts of NO released from glut-DNICs added to plasma or aqueous buffer were quantitatively similar, we observed notable qualitative changes in the peak shapes following addition of DNICs to plasma. As shown in Figure 2A and B, glut-B and MDNICs added to plasma prior to injection into triiodide had a more rapid NO release than glut-MDNICs added to water, as demonstrated by sharper, taller peak profiles in the plasma samples. The change in peak profile occurred within 30 seconds after addition of glut-MDNICs to ice-cold plasma, but occurred more gradually over ~10 minutes for glut-BDNICs. Similar changes in peak profile were also observed in the Ac/FeCN and PBS/FeCN reagents (data not shown). The change in peak shape was not associated with any change in total NO_X released from the DNICs, and seems likely to have been due to conversion of the low molecular weight glut-DNICs to high molecular weight protein-liganded MDNICs. Such conversion has previously been reported to occur quantitatively at higher temperatures [19]. We found this conversion to be temperature-dependent for BDNICs as well, such that the change in peak profile was complete in less than 30 seconds when samples were at 37°C (data not shown).

To further test this possible conversion we performed experiments to separate low and high molecular weight DNICs prior to injection into the purge vessel reagents. Low molecular weight glut-B- or MDNIC standards were diluted into plasma (1:9 final concentration 100 μM), and incubated at 37°C for five minutes to promote the full conversion of low molecular weight DNICs to high molecular weight. The plasma solution was then passed through a 5 kD molecular weight cutoff size-exclusion G25 column, from which fractions were collected and assayed for NOx metabolites by PBS/FeCN and Ac/FeCN reagents. Consistent with complete transformation of the glut-DNICs into high molecular weight DNICs, the PBS/FeCN reagent (which detects only DNICs) produced signals only from the high molecular weight fractions (fractions 1 to 12, Figure 2E). Also consistent with the change in peak shapes observed and described above, after 5-mins of incubation in plasma the obtained DNIC gave sharper, nitrite-like, peaks in triiodide, Ac/FeCN and PBS/FeCN with no apparent change in concentration compared to water, but seems to be slightly more sensitive to detection by Ac/Asc (Figure S8). Similar to the observations for DNIC transformations on ice, the increase in DNIC sensitivity in the triiodide, Ac/FeCN, and PBS/FeCN, does not result in the change of measured concentrations as shown in Figure S8. Additionally, peaks obtained from the high molecular weight fractions were sharper than those of the low molecular weight glut-DNIC standards (data not shown), again suggestive of more rapid release of NO from the high molecular weight DNICs in the PBS/FeCN reagent. The Ac/FeCN assay, which detects both nitrite and DNICs, measured significant amounts of low molecular weight NOx (fractions 13 to 25) presumably due to nitrite contamination in the stock glut-DNICs, and also possibly due to metabolism of the DNICs into nitrite during the 5-minute incubation period.

Another notable characteristic of peak shape was observed with the Ac/Asc assay. Upon injection of DNICs, whether in plasma or aqueous buffer, small sharp peaks corresponding to nitrite contamination in the DNICs were observed, as described above. The chemiluminescence signal failed to return to baseline following these sharp peaks, instead remaining slightly elevated (Figure 2C and D). This is presumably due to a slow release of NO from the DNICs in the Ac/Asc reagent. Importantly, however, the AUC of the sharp portion of the peaks was the same whether the DNICs were in plasma or deionized water solutions (Figure 2C). Thus, by selecting only the initial sharp portion of the curve the assay can still be used to distinguish reliably between DNICs and nitrite in both deionized water and plasma solutions, although accurate determination of the endpoint of the nitrite peak requires particular attention.

Linearity and specificity of assays in mixtures of NOx species

After characterizing the specificity of the different reagents for 10 mM glut-DNICs, nitrite, and GSNO individually, we next evaluated the linearity of the assay across a range of concentrations for each NOx species by generating linear regressions of peak areas obtained from injections of standards at concentrations ranging from 0 to 10 mM. Regression plots were prepared for NOx species in both water and plasma to capture matrix-specific effects. Since DNICs, nitrite, and SNOs are likely to co-exist in biological samples [4], we also determined whether the presence of 10 mM nitrite and GSNO in the sample would affect the measured release of NO from DNICs. Plots of each standard curve are presented in the Supplemental information.

Nitrite yielded matching curves in plasma and deionized water in the triiodide and Ac/Asc reagents (Figure S6A, B) with high linearity (r^2 = 0.9998, and 0.9987 in water and plasma respectively). The slopes and intercepts of these curves were also similar, demonstrating that nitrite measurements in the triiodide or Ac/Asc reagents are comparable in both deionized water and plasma solutions. As expected, the concomitant presence of 10 μM DNICs or GSNO resulted in a significant elevation of the y-intercept in the triiodide assay. However, the quantitative release of NO from nitrite was not affected, as demonstrated by the similar slopes in the presence and absence of DNICs or GSNO (Figure S6C, D). In plasma, the concomitant presence of GSNO in the nitrite samples also did not interfere with the quantitative release of NO from nitrite in the Ac/Asc reagent (Figure S6C). In contrast, however, the presence of DNICs did result in a ~13% increase in the slope of the nitrite standard curve in the Ac/Asc assay with no effect on the y-intercept (Figure S6E, F). The increase in slope without a shift in the y-intercept in the presence of 10 mM DNICs is most likely attributable to an artifactual overestimation of the nitrite peak area caused by the slow release of NO from DNICs that resulted in a failure of the peaks to return completely to baseline (described above). Another possible explanation is partial degradation of the low molecular weight DNICs to nitrite in plasma, although this seems less likely due to the similar y-intercepts.

As described above, the Ac/FeCN assay detected nitrite and DNICs but not GSNO. This assay was linear for both nitrite and glut-B- and MDNICs, and also maintained its specificity

for nitrite and DNIC measurement in the presence of 10 μM GSNO in plasma (Figure S7A-D).

The PBS/FeCN assay detected DNICs but not nitrite or GSNO (see above). Standard curves for glut-B and MDNICs were linear in both aqueous buffer and plasma, indicating quantitative release of NO from the DNICs in both matrices from 0 to 10 mM. In the presence of 10 mM nitrite and GSNO. The assay maintained its specificity for DNIC measurement in the presence of an equimolar mixture of 10 μM nitrite and GSNO (Figure S7E, F).

It should be noted that while the PBS/FeCN reagent selectively detects DNICs in the presence of nitrite and SNOs, it is not expected to be selective against other forms of iron nitrosyl (FeNO) such as heme nitrosyls (heme-NO) [3]. Although differentiating between types of FeNO was not a major focus of the current work, we did note that the Ac/Asc assay quantitatively detects heme-NO in addition to nitrite, but does not detect DNICs as shown in Figure 5E. This result was also reported by Nagababu et al. who explained that the low pH of the acetic acid, not the ascorbic acid, is responsible for the observed NO release [25]. The peak resulting from NO release from heme-NO in Ac/Asc is broad and qualitatively different from the sharp peak observed when either nitrite or nitrite-contaminated DNICs are injected into a purge vessel with Ac/Asc. This difference allows for discrimination between DNICs and heme-NO since both are detectable by PBS/FeCN but only the heme-NO is detectable by Ac/Asc.

Quantification of DNICs in the presence of nitrite and SNOs

A potential usefulness of the present assays lies in their ability to selectively quantify concentrations of mixtures of DNICs, nitrite, and SNOs in biological samples. As summarized in Figure 3, this can be accomplished for nitrite and DNICs by direct measurement, and for RSNOs by deduction based on the results from two different assays. Figure 3 therefore demonstrates the feasibility of using these assays to quantify unknown concentrations of these NOx species, as applied and reported in the results section for the rats exposed to LPS (“Effect of LPS-stimulation on NOx species in rat tissues”). Concentrations of the specific NOx species calculated from rat liver homogenates after LPS-treatment are shown in Table S2 of the supplementary information.

Detection of LPS-stimulated DNIC in RAW 264.7 macrophages

Having demonstrated the selectivity of the assays in water and plasma, we next used them to measure NOx concentrations in cultured cells before and after stimulation of endogenous NO production. Treatment of RAW 264.7 macrophages with lipopolysaccharide (LPS) has been found previously to stimulate overproduction of NO by iNOS, resulting in DNIC formation as measured by EPR, as well as nitrite due to oxidation of NO [4, 22, 28]. We therefore employed the selective assay reagents to measure NOx levels of LPS-stimulated RAW 264.7 macrophages and thereby test for formation of various NOx species. Following exposure of the cultured macrophages to LPS, culture media and cell lysates were collected into separate aliquots for NOx determination (Figure 4). Consistent with upregulation of iNOS activity, LPS stimulation resulted in an increase in total NOx levels in the culture

media as measured by the triiodide assay (Figure 4A) from 0.45 ± 0.01 μM in non-LPS-stimulated controls to 15.7 ± 0.4 μM with LPS stimulation. PBS/FeCN detected nothing in media from control cells, but 0.06 ± 0.01 μM in LPS-stimulated cells (Figure 4B). Our detection of extracellular DNICs provides further, to the best of our knowledge, the first direct experimental evidence to the hypothesis by Richardson and coworkers that low molecular weight DNICs are the transport form of iron, and are released extracellularly during the iron efflux observed after the exposure of nitric oxide to different cell lines [9–12]. The ~ 0.1 μM DNIC signal that we detect after injection of 500 mL sample to the purge vessel (~50 pmol NO equivalence) also highlights the improved sensitivity of chemiluminescence in contrast to EPR, based on a 1 mM MDNIC sensitivity (250 uL sample, 2 NO per MDNIC = 500 pmol NO equivalence) [29].

Stimulation of macrophages with LPS also increased intracellular NO_x levels. As expected from previous reports, both total NOx (Figure 4C) and intracellular DNIC concentrations (Figure 4D) were increased in a manner dependent on LPS dose [28, 29]. When normalized to total protein concentrations, DNICs comprised approximately 2% of the total NOx species in the cell lysates. In contrast to our result, Hickok et al found DNICs to be the predominant intracellular NOx species [28]. This difference likely reflects sample handling differences in our respective studies. Unlike Hickok et al who measured DNICs by EPR in snap frozen cells without thawing, measuring DNICs by chemiluminescence requires that we first thaw the cells. We therefore lysed macrophages by repeated freeze-thaw under ambient oxygen levels, which could have promoted metabolism of DNICs into nitrite and/or nitrosothiols. It is therefore possible that we underestimated the intracellular ratio of DNICs to other NOx. Future studies are needed to determine the ideal sample preparation protocols which best preserve DNICs for assay. The LPS and iron dose-dependency of DNIC formation is shown in Figure S12, while Figure S11 shows the peak shape of the detected signal in the PBS/FeCN assay. DNIC formation was not observed in alpha-MEM media regardless of successful iNOS stimulation as shown in Figure S13.

Effect of LPS-stimulation on NOx species in rat tissues.

Having successfully measured DNICs in water, plasma, and cell lysates, we next applied the assays to rat tissues. Using EPR, previous studies have demonstrated that DNICs are formed in rat tissue after exposure of the animal to bacterial lipopolysaccharide (LPS) [5, 30]. Based on this evidence, we injected rats with LPS, sacrificed them after six hours, and assayed plasma, whole blood, and liver tissue samples for NOx levels with the different purge vessel reagents to determine whether our methods could detect DNICs in agreement with previous studies.

The rats responded to LPS injection with a transient drop in body temperature measured two hours after injection (Figure 5A), a response that is typical for rats given LPS [20, 30]. Further confirmation of successful LPS treatment was indicated by an increase in plasma and whole blood total NOx levels compared to controls (10.7 ± 1.6 vs. 0.14 ± 0.01 .μM, and 18.8 ± 2.9 vs. 0.04 ± 0.02 μM for plasma and whole blood respectively, Figure 5B, C). These increases are consistent with stimulated iNOS activity as reported previously [31–33].

The NO_x concentrations deduced from the selective assays are shown in Figure 5. In the plasma most of the NOx was in the form of nitrite (8.3 ± 1.2 μM) as determined by the Ac/Asc assay, with significant amounts of SNO (3.8 ± 0.8 μM) also present as deduced from the difference between the triiodide and the Ac/FeCN signal. Smaller amounts of plasma FeNOs (0.49 ± 0.09 μM) were found as determined by the PBS/FeCN assay. In whole blood, larger total NO_x concentrations were found than in plasma (18.8 ± 2.9 μM vs. 10.7 ± 1.5 μM) as determined by the triiodide assay. About half of the whole blood total NOx was in the form of FeNOs (10.8 ± 3.0 μM) as determined by the PBS/FeCN assay. The FeNOs detected by the PBS/FeCN assay in whole blood are most likely iron nitrosylated hemoglobin (HbNO), not DNICs, due to the abundance of hemoglobin in the red blood cell. Previous studies using EPR have also shown that HbNO levels are elevated during endotoxemia in rats [30].

LPS treatment also resulted in increased NOx levels in the liver (from 6.1 ± 3.8 to 100 ± 26 pmol/mg-protein, Figure 5D). Nearly all the NOx in the liver was in the form of FeNOs, based on the insignificant difference between the NO_x levels measured by the triiodide assay, which detects all NO_x species (except nitrate), and the PBS/FeCN assay which only detects FeNOs. Detection of NO_x in liver tissue homogenates by the Ac/Asc assay revealed NOx levels that were equal to those measured by both the triiodide and PBS/FeCN assays (Figure 5E, F), and peaks that were qualitatively like the HbNO standards. Thus, given that the Ac/Asc assay detects heme-NO but not DNICs, the FeNO detected in the liver tissue was most likely heme-NO. This result would be anticipated considering the high heme concentrations of the liver. We measured the total heme concentrations to be an order of magnitude higher than FeNO concentrations in both control and LPS-treated rats (~10,000 pmol/mg protein, Figure S7), which makes it plausible that heme-NO was a significant portion of the FeNO signal. FeNOs, most likely heme-NO, are also formed upon treatment of liver homogenates with exogenous NO derived from ProliNONOate as demonstrated in Figure S9. It is however worth noting that Thomas et al. have recently found that the rat liver has at least 8-fold higher concentrations of DNICs, measured by EPR, compared to NO detected via a ferricyanide-based chemiluminescence assay, which they specified as heme-nitrosyl [34]. Since we demonstrate that the ferricyanide assay can quantitatively release NO from both B- and MDNICs as well as heme-nitrosyl, and since EPR detects only MDNICs, one might expect their chemiluminescence concentrations to be at least equal to or higher than their EPR concentrations. This apparent discrepancy may be ascribed to potential loss of DNICs during sample handling, since the chemiluminescence measurements require a longer sample processing time with an intermediary thawing step, which is not required for EPR. It is also possible that differences in the calibration of EPR compared to chemiluminescence could also explain this difference. Further cross-validation of EPR and chemiluminescence methods, with characterization of the stability of DNICs in various tissue types and sample preparation protocols, is necessary in order to more fully understand results that have been obtained with these two methods.

4. Discussion

We have developed chemiluminescence-based methods for selective detection of both low and high molecular weight DNICs in the presence of nitrite and nitrosothiols, in both water/

buffer and biological media. These methods have a broad linear range, are highly reproducible (Table S1), have lower limits of detection and quantification that extend more than an order of magnitude below the reported capacity of the gold-standard EPR method, and are effective for both MDNICs and EPR-silent BDNICs.

Due to their unique molecular structure and stability, thiolate DNICs are emerging as important links in the crosstalk between NO, iron and thiol signaling pathways. DNICs have been suggested to play several roles, including as intracellular storage forms of NO under conditions of excess NO production [8], mediating iron-efflux from cells after exposure to NO [9–12], and exerting anti-oxidative effects in inflammatory cells by scavenging chelatable iron [18, 35, 36]. Formation of DNICs has been associated with inhibition of caspase-3 activity due to nitrosylation of the caspase-3 cysteine residues, leading to a reduction of apoptosis [22]. DNICs also have vasodilatory effects [8, 13], and a glutathione-based DNIC is currently in clinical trials as a long-lasting NO-donor for the treatment of systemic hypertension [14]. However, DNICs are still much understudied compared to other NO adducts, partly due to limitations in DNIC-detection techniques. And indeed their concentration and function under physiological conditions remain a matter of controversy and uncertainty.

Virtually all published measurements of DNICs have been performed with EPR, which has lower limits of detection that are above concentrations of DNICs known to be bioactive, thus hindering the ability to study the physiological role of DNICs. Furthermore, EPR detects only the paramagnetic MDNICs and not the diamagnetic BDNICs, a particularly important limitation given recent work by Vanin and coworkers suggesting that BDNICs are a prevalent form of DNIC in tissues [5]. Recent work by Hogg and coworkers has also attempted to solve the paucity of methods that can detect DNICs through use of HPLC/spectrophotometry, and a limited attempt at using chemiluminescence to indirectly infer the presence of thiolate DNICs [4]. Our work is the first to use chemiluminescence to directly measure thiolate DNICs in both deionized water and biological media, to discriminate between thiolate DNICs, nitrite, and nitrosothiols without the need for sample processing with pretreatment reagents, to demonstrate the high molecular weight nature of plasma DNICs, and to preliminarily characterize the different NO-release behavior of low molecular weight vs. high molecular weight DNICs when release is brought about by different purge vessel solutions.

The PBS/FeCN assay is ideal for DNIC detection since it directly measures NO release from DNICs without interference from nitrite. This assay is compatible with plasma, whole blood, cell media, cell lysates, tissue homogenates, and supernatants from tissue homogenates. The main limitation of this assay is that it indiscriminately detects NO from oxidizable NOx species such as heme nitrosyl groups (e.g. HbNO used for the assay's calibration), and nitroxyl (HNO). The assay would therefore be more useful for specific DNIC detection in systems where significant iron nitrosyl species are not expected, or where the concentrations of these iron nitrosyl species can be independently determined. In the presence of iron nitrosyls, DNIC concentrations can be estimated by the in-tandem use of the PBS/FeCN assay, the Ac/FeCN assay, and the Ac/Asc assay due to the ability of Ac/Asc to quantitatively detect heme-iron, and its partial and very slow degradation of DNICs. As for

HNO, there is currently little evidence that it plays a significant physiological role [37]. However due to the non-innocent nature of NO as a ligand [38–40], it is difficult to determine the exact oxidation state of the central iron, or the NO in DNICs, such that it is possible that DNICs themselves could act as nitroxyl donors if the NO in the DNICs is in the NO^- form, as proposed by some investigators [41–43]. This would make it harder to differentiate whether DNICs are releasing NO in FeCN due to the oxidation of the Fe^{2+} center, or due to the oxidation of a nitroxyl intermediate, or the direct oxidation of an iron-bound nitroxyl moiety. In addition to the unclear nature of the oxidation state of iron or NO in DNICs, it is also surprising that both a strong reducing agent (triiodide) and a strong oxidizing agent (ferricyanide) can equally release NO from DNICs. Future work, maybe by first studying the oxidation/reduction potentials of DNICs under different conditions, might be able to yield mechanistic insight on how this NO release from DNICs by triiodide and ferricyanide occurs.

The combination of our methods makes it possible to discriminate between thiolate DNICs, nitrite and nitrosothiols. Nitrite and nitrosothiols are synthetic contaminants of thiolate DNICs, degradation products of DNICs, and more significantly, the main products of NO metabolism and thus expected to coexist with DNICs intracellularly. Previous methods have used different pretreatment reagents such as acidified sulfanilamide and mercury chloride to discriminate between nitrite and nitrosothiols, without regard for the possible impact of these reagents on DNICs [24]. For this study, we mostly avoided the use of pretreatment reagents due to our unpublished observations with spectrophotometry, EPR and chemiluminescence that both mercury chloride and acidified sulfanilamide cause the degradation and/or transformation of both glut-DNICs and protein-bound DNICs. In line with these observations, Keszler et al. recently reported that DNICs are sensitive to mercury chloride reduction [4], which strengthens the need for selective NO-detection techniques that do not rely on sample processing with pretreatment reagents. Importantly, the instability of DNICs in the presence of commonly-used pretreatment reagents such as acid sulfanilamide and mercury chloride raises the possibility that previous reports may have overestimated nitrite and nitrosothiol concentrations and overlooked significant levels of DNICs.

To avoid the use of pretreatment reagents we therefore utilized purge vessel reagents first developed by Rifkind and Nagababu for the selective determination of nitrite, nitrosothiols or FeNOs [1–3, 25, 27]. To our knowledge, the current work is the first to optimize and validate these methods for detection of DNICs, or for selectivity against DNICs, and to combine their use to decipher the identity of NOx species in biological samples. For instance, we have validated that the Acetic/FeCN assay measures nitrite and both high and low molecular weight DNICs without interference from nitrosothiols. Previous work by Rifkind and Nagababu employed acidified sulfanilamide to remove the nitrite from samples prior to injection into the purge vessel, which allowed the assay to only detect FeNOs, including DNICs [3]. To avoid sample preprocessing with chemical reagents, we however suggest determination of FeNOs from the difference in NO released from the Ac/Asc reagent, which is nitrite-specific, and the Acetic/FeCN reagent, which measures nitrite and FeNOs, to allow subtraction of the nitrite signal from the combined nitrite and FeNO signal. The simultaneous use of the Acetic/FeCN assay and the triiodide assay can also be used to approximate nitrosothiol concentrations, with greater accuracy especially where other

triiodide detectable NOx species such as nitrosamines are not expected. Nitrosothiol concentrations can also be estimated from the difference between the chemiluminescence signal of the assay with Cu(II) in Ac/Asc, which detects nitrosothiols and nitrite, and the Ac/Asc assay which detects only nitrite. However, the assay with Cu(II) in Ac/Asc needs to be further optimized for better compatibility with plasma or high protein samples.

Although this study is the first to validate the ability to measure DNICs with ozone-based chemiluminescence, several limitations should be noted. First, the stability of DNICs in various biological matrices must be taken into account. The stability of DNICs could depend on parameters such as type of fluid/tissue, oxygen levels, and presence of metal chelators or oxidizing agents in the matrix, as currently being studied in our lab. These considerations merit fast sample preparation, but also increases the possibility that the current method could underestimate DNIC concentrations. Second, although the PBS/FeCN reagent detects DNICs quantitatively, it cannot distinguish between DNICs and other types of FeNO such as heme nitrosyls. This limitation may be at least partially overcome by the finding that the Asc/Ac assay detects heme-NO but not DNICs, but further validation using methods that can clearly distinguish between various FeNO species is required. Third, the current validation has been based on the use of stock solutions of nitrosothiols and DNIC synthesized with glutathione as the thiolate ligand. Although we demonstrate that these stock NOx species rapidly convert to high molecular weight species, the approach does not account for the possibility of differences in the detectability of all the various naturally-occurring nitrosothiols and DNICs. Fourth, the current work focuses solely on thiolate-DNICs. DNICs have been reported to be bound to peptide or protein histidinyl ligands, and to tyrosine, serine and threonine residues of proteins, or with mixed ligands [7, 44]. Whether these non-thiolate DNICs exhibit similar detectability remains to be determined.

One of the points to be drawn from this study is the effect of ferricyanide on DNICs. Since we demonstrate that ferricyanide promotes the release of NO from DNICs at both low and neutral pH, it is possible that use of ferricyanide in nitrite-preserving solutions commonly used during sample collection potentially results in the loss of any DNICs present in the sample.

Conclusions

Chemiluminescence is a well-established and extremely sensitive technique for the detection of NO and many of its metabolites. We have combined the power of ozone-based chemiluminescence with the knowledge of selective NO-releasing reagents to yield assays that cannot only detect DNICs in biological matrices, but can also be used in the discrimination of key NO metabolites. The methods that we developed can be used in tandem with existing methods such as EPR, for DNIC detection, or can be used independently where interferences are not expected.

Supplementary Material

Refer to Web version on PubMed Central for supplementary material.

Acknowledgements

We thank Shannon Bragg for assistance with rat surgeries.

This project was supported by grants from the NIH (R01 HL95973 to ABB and R01 HL119280 to TEP).

References

1. Nagababu E and Rifkind JM, Measurement of plasma nitrite by chemiluminescence. Methods Mol Biol, 2010 610: p. 41–9. [PubMed: 20013171]
2. Nagababu E and Rifkind JM, Determination of s-nitrosothiols in biological fluids by chemiluminescence. Methods Mol Biol, 2011 704: p. 27–37. [PubMed: 21161627]
3. Nagababu E, et al., Active nitric oxide produced in the red cell under hypoxic conditions by deoxyhemoglobin-mediated nitrite reduction. J Biol Chem, 2003 278(47): p. 46349–56. [PubMed: 12952953]
4. Keszler A, et al., Thiolate-based dinitrosyl iron complexes: Decomposition and detection and differentiation from S-nitrosothiols. Nitric Oxide, 2017 65: p. 1–9. [PubMed: 28111306]
5. Mikoyan VD, et al., The binuclear form of dinitrosyl iron complexes with thiol-containing ligands in animal tissues. Nitric Oxide, 2017 62: p. 1–10. [PubMed: 27989818]
6. Graziano M and Lamattina L, Nitric oxide and iron in plants: an emerging and converging story. Trends Plant Sci, 2005 10(1): p. 4–8. [PubMed: 15642517]
7. Boese M, et al., S-Nitrosation of Serum Albumin by Dinitrosyl-Iron Complex. Journal of Biological Chemistry, 1995 270(49): p. 29244–29249. [PubMed: 7493954]
8. Mulsch AMP, Vanin AF, Busse R, The potent vasodilating and guanylyl cyclase activating dinitrosyl-iron(II) complex is stored in a protein-bound form in vascular tissue and is released by thiols. FEBS Lett. , 1991 294(3): p. 252–256. [PubMed: 1684553]
9. Suryo Rahmanto Y, et al., Nitrogen monoxide (NO) storage and transport by dinitrosyl-dithiol-iron complexes: long-lived NO that is trafficked by interacting proteins. J Biol Chem, 2012 287(10): p. 6960–8. [PubMed: 22262835]
10. Watts RN, et al., Nitrogen monoxide (NO)-mediated iron release from cells is linked to NO-induced glutathione efflux via multidrug resistance-associated protein 1. Proceedings of the National Academy of Sciences, 2006 103(25): p. 9744–9744.
11. Lok HC, et al., Glutathione S-transferase and MRP1 form an integrated system involved in the storage and transport of dinitrosyl-dithiolato iron complexes in cells. Free Radic Biol Med, 2014 75: p. 14–29. [PubMed: 25035074]
12. Lok HC, et al., Nitric oxide storage and transport in cells are mediated by glutathione S-transferase P1–1 and multidrug resistance protein 1 via dinitrosyl iron complexes. J Biol Chem, 2012 287(1): p. 607–18. [PubMed: 22084240]
13. Vanin AFMV, Serezhenkov VA, Chazov EI, Vasorelaxing activity of stable powder preparations of dinitrosyl iron complexes with cysteine or glutathione ligands. Nitric Oxide, 2007 16(3): p. 322–30. [PubMed: 17258478]
14. Timoshin AA, et al., The hypotensive effect of the nitric monoxide donor Oxacom at different routs of its administration to experimental animals. Eur J Pharmacol, 2015 765: p. 525–32. [PubMed: 26376026]
15. Tonzetich ZJ, McQuade EL, and Lippard JS , Detecting and Understanding the Roles of Nitric Oxide in Biology. Inorg Chem, 2010 49(14): p. 6338–6348. [PubMed: 20666391]
16. Borodulin RR, et al., A simple protocol for the synthesis of dinitrosyl iron complexes with glutathione: EPR, optical, chromatographic and biological characterization of reaction products. Nitric Oxide, 2013 35: p. 110–5. [PubMed: 24018466]
17. Broniowska KA, Diers AR, and Hogg N, S-nitrosoglutathione. Biochim Biophys Acta, 2013 1830(5): p. 3173–81. [PubMed: 23416062]
18. Li Q, et al., Nitrosothiol formation and protection against Fenton chemistry by nitric oxide-induced dinitrosyliron complex formation from anoxia-initiated cellular chelatable iron increase. J Biol Chem, 2014 289(29): p. 19917–27. [PubMed: 24891512]

19. Timoshin AA, et al., Distribution and pharmacokinetics of dinitrosyl iron complexes in rat organs. Biophysics, 2012 57(2): p. 233–236.
20. Kaplanski J, N. A, Sharon-Grannit Y , Lithium attenuates lipopolysaccharide-induced hypothermia in rats. European Review for Medical and Pharmacological Sciences, 2014 18: p.1829–1837. [PubMed: 24992627]
21. Bradford M, A rapid and sensitive method for the quantitation of microgram quantities of protein utilizing the principle of protein-dye binding. Analytical Biochemistry, 1976 72: p. 248–54. [PubMed: 942051]
22. Kim Y-M, Cellular Non-heme Iron Content Is a Determinant of Nitric Oxide-mediated Apoptosis, Necrosis, and Caspase Inhibition. Journal of Biological Chemistry, 2000.
23. Samuilov A and Zweier JL, Development of Chemiluminescence-Based Methods for Specific Quantitation of Nitrosylated Thiols. Analytical Biochemistry, 1998 258: p. 322–30. [PubMed: 9570848]
24. Wang X, et al., Measurement of nitric oxide levels in the red cell: validation of tri-iodide-based chemiluminescence with acid-sulfanilamide pretreatment. J Biol Chem, 2006 281(37): p. 26994–7002. [PubMed: 16845122]
25. Nagababu E and Rifkind JM, Measurement of plasma nitrite by chemiluminescence without interference of S-, N-nitroso and nitrated species. Free Radic Biol Med, 2007 42(8): p. 1146–54. [PubMed: 17382196]
26. Almeida LE, et al., Validation of a method to directly and specifically measure nitrite in biological matrices. Nitric Oxide, 2015 45: p. 54–64. [PubMed: 25445633]
27. Salgado MT, et al., Red blood cell membrane-facilitated release of nitrite-derived nitric oxide bioactivity. Biochemistry, 2015 54(44): p. 6712–23. [PubMed: 26478948]
28. Hickok JR, et al., Dinitrosyliron complexes are the most abundant nitric oxide-derived cellular adduct: biological parameters of assembly and disappearance. Free Radic Biol Med, 2011 51(8): p. 1558–66. [PubMed: 21787861]
29. Hickok JR, et al., Nitric oxide suppresses tumor cell migration through N-Myc downstream-regulated gene-1 (NDRG1) expression: role of chelatable iron. J Biol Chem, 2011 286(48): p. 41413–24. [PubMed: 21976667]
30. Bergamini S, et al., N-acetylcysteine inhibits in vivo nitric oxide production by inducible nitric oxide synthase. Nitric Oxide, 2001 5(4): p. 349–60. [PubMed: 11485373]
31. Schweighöfer H, C. R ,Mayer K, Rosengarten B, Brain function in iNOS knock out or iNOS inhibited (l-NIL) mice under endotoxic shock. Intensive Care Medicine Experimental, 2014 2: p. 24. [PubMed: 26266921]
32. Galleano M, Simontacchi M, and Puntarulo S, Nitric oxide and iron: effect of iron overload on nitric oxide production in endotoxemia. Mol Aspects Med, 2004 25(1–2): p. 141–54. [PubMed: 15051323]
33. Jang KJ, et al., Anti-inflammatory potential of total saponins derived from the roots of Panax ginseng in lipopolysaccharide-activated RAW 264.7 macrophages. Exp Ther Med, 2016 11(3): p. 1109–1115. [PubMed: 26998045]
34. Thomas DD, et al., Differential mitochondrial dinitrosyliron complex formation by nitrite and nitric oxide. Redox Biol, 2018 15: p. 277–283. [PubMed: 29304478]
35. SERGENT O, et al., Effect of Nitric Oxide on Iron-Mediated Oxidative Stress in Primary Rat Hepatocyte Culture. Hepatology, 1997 25: p. 127.
36. Gorbunov N, et al., Nitric Oxide Prevents Oxidative Damage Produced by tert-Butyl Hydroperoxide in Erythroleukemia Cells via Nitrosylation of Heme and Non-heme Iron. Journal of Biological Chemistry, 1997 272(19): p. 12328–12341. [PubMed: 9139677]
37. Switzer CH, et al., The emergence of nitroxyl (HNO) as a pharmacological agent. Biochim Biophys Acta, 2009 1787(7): p. 835–40. [PubMed: 19426703]
38. Broclawik E, Stepniewski A, and Radon M, Nitric oxide as a non-innocent ligand in (bio-)inorganic complexes: spin and electron transfer in Fe(II)-NO bond. J Inorg Biochem, 2014 136: p. 147–53. [PubMed: 24495545]
39. Paolocci N, et al., The pharmacology of nitroxyl (HNO) and its therapeutic potential: not just the Janus face of NO. Pharmacol Ther, 2007 113(2): p. 442–58. [PubMed: 17222913]

40. Staurengo-Ferrari L, et al., The nitroxyl donor Angeli's salt ameliorates Staphylococcus aureus-induced septic arthritis in mice. Free Radic Biol Med, 2017 108: p. 487–499. [PubMed: 28419865]

41. Shumaev KB, et al., New dinitrosyl iron complexes bound with physiologically active dipeptide carnosine. J Biol Inorg Chem, 2017 22(1): p. 153–160. [PubMed: 27878396]

42. Ye S and Neese F, The Unusual Electronic Structure of Dinitrosyl Iron Complexes. Journal of American Chemical Society, 2010 132: p. 3646–3647.

43. Tseng YT, et al., To Transfer or Not to Transfer? Development of a Dinitrosyl Iron Complex as a Nitroxyl Donor for the Nitroxylation of an Fe(III) -Porphyrin Center. Chemistry, 2015 21(49): p. 17570–3. [PubMed: 26437878]

44. De Maria F, et al., The specific interaction of dinitrosyl-diglutathionyl-iron complex, a natural NO carrier, with the glutathione transferase superfamily: suggestion for an evolutionary pressure in the direction of the storage of nitric oxide. J Biol Chem, 2003 278(43): p. 42283–93. [PubMed: 12871945]

Highlights

- • Use of different purge vessel reagents enables selective quantification of specific classes of NOx species in a biological matrix
- • O_3-based chemiluminescence with ferricyanide in PBS detects both binuclear and mononuclear DNICs selectively from nitrite and nitrosothiols
- • As low as 25 pmol NO released from DNICs can be detected, which is ≥10-fold more sensitive than currently available methods
- • Glutathione-liganded DNICs rapidly convert to high molecular weight DNICs in plasma

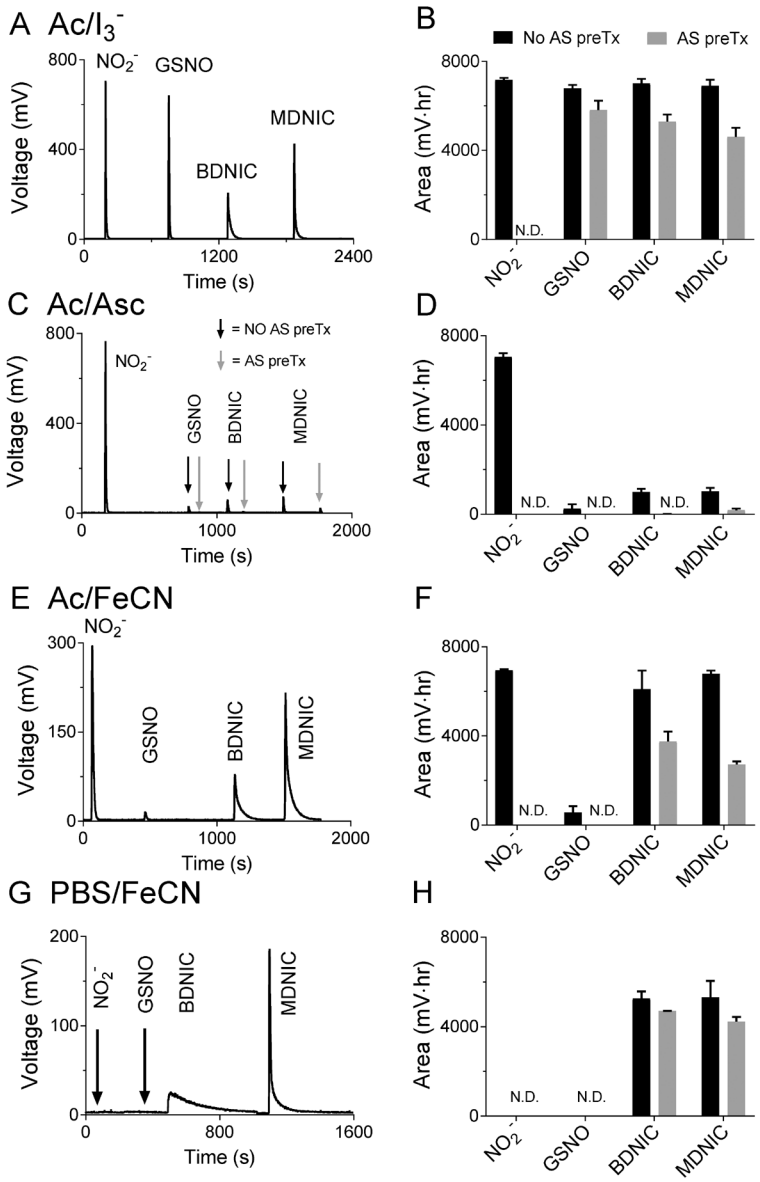

Figure 1.

Representative traces showing peak profiles of NO released from plasma solutions of DNICs, nitrite and GSNO in different reagents, as well as the corresponding peak areas. The different reagents used are: Ac/I3 (A, B), Ac/Asc (C, D), Ac/FeCN (E, F), and PBS/FeCN (G, H). On four different days 1000 pmol of each NO-adduct was injected into the purge vessel for all assays with fresh NO-adduct aliquots to give $n = 4$. All concentrations are given with respect to the NO equivalence to allow release of the same amount of NO from different molecules (1000 pmol MDNIC = 500 pmol MDNIC by molecule, 1000 pmol BDNIC = 250 pmol by molecule). All reactions were carried out with the purge vessel at room temperature. Note the PBS/FeCN assay is selective for DNICs (G, H). Also note the loss of DNIC signal following acid sulfanilamide (AS) treatment in the Ac/FeCN (F) and PBS/FeCN (H) assays, which is attributed to nitrite contamination and DNIC degradation as

discussed in the text. For the AS pretreatment, 80 mL of sample was added to a vial with 20 mL of 2.5% w/v AS in 1 M HCl.

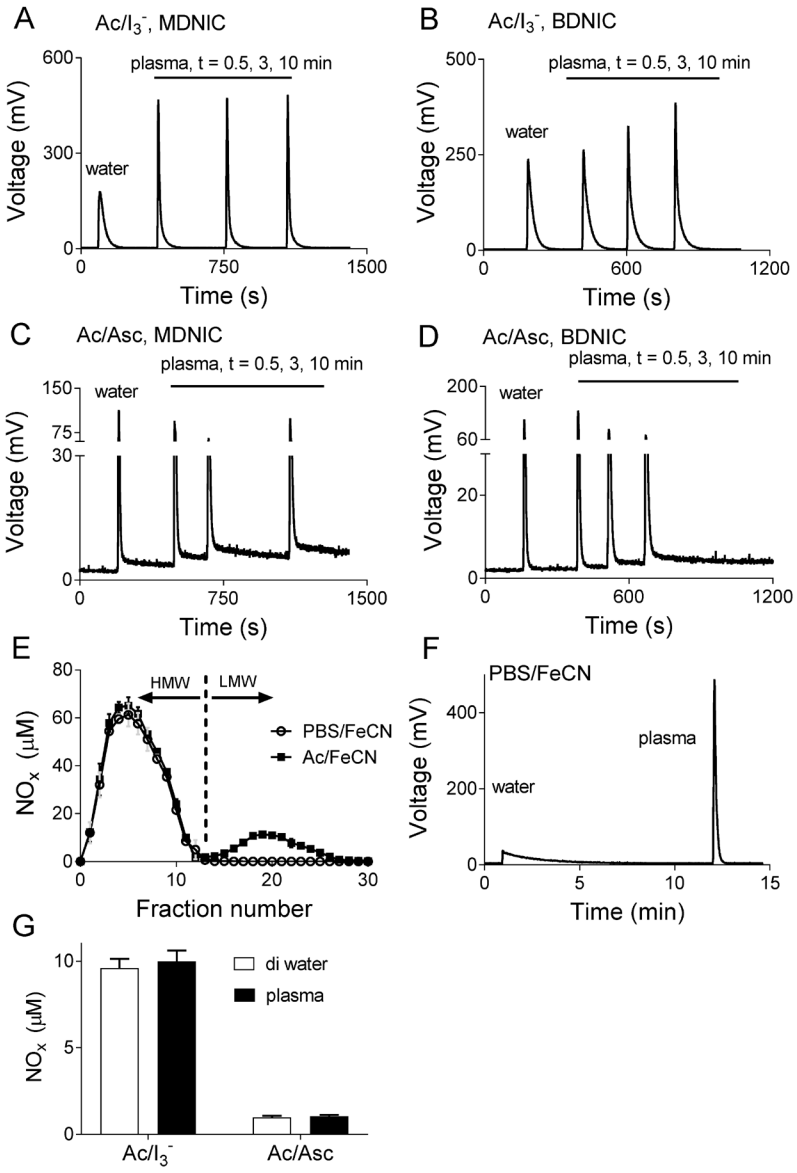

Figure 2.

Representative peak profiles of low molecular weight DNICs comparing water and plasma in triiodide for total NOx (DNIC and nitrite/nitrosothiol contamination) (A, B), and ascorbic acid for nitrite (C, D) determination. The close agreement between NOx concentrations from plasma and water DNIC samples indicates plasma constituents do not influence NO release in these assays. Note the elevated baseline that is observed after injection of plasma DNICs in the Ac/Asc assay indicating the presence of a slow NO release species in plasma. The plasma DNICs were kept on ice for all the time points to minimize metabolic changes. n =3. E) Transformation of low molecular weight BDNICs into high molecular weight DNICs. Low molecular weight DNICs were added to plasma and allowed to equilibrate for 5 mins at 37 °C. The mixture was then passed through a G-25 column and fractions collected. The high molecular weight fraction (>5 kDa) elutes first, followed by the low molecular weight fractions (fraction number >12 for BDNIC). Both low molecular weight glut-B and glut-

MDNIC (not shown) can be seen to be converted into high molecular weight DNICs. F) Peak profiles of low molecular weight glut-BDNIC in deionized water, and the corresponding high molecular weight plasma DNICs in PBS/FeCN. Plasma DNIC show faster NO-release compared to BDNICs in deionized water in the PBS/FeCN, triiodide and Ac/FeCN assays. G) Total NOx and nitrite concentrations of a 10 μM B- and MDNIC equimolar mixture, as measured by Ac/I3- and Ac/Asc for the peaks shown in A-D. The change in DNIC peak profile does not change the integrated concentrations.

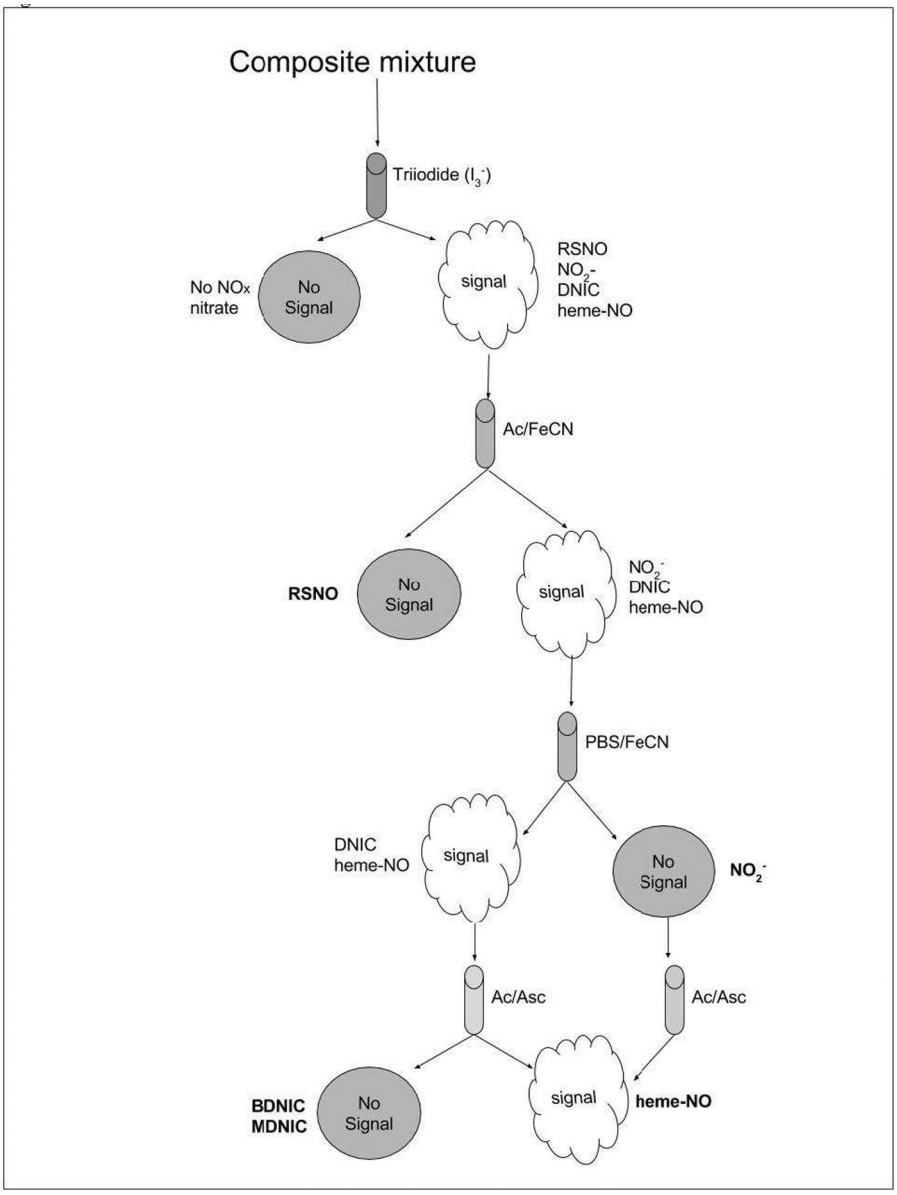

Figure 3.

Illustration of how combined use of different chemiluminescent purge vessel reagents can allow the characterization and quantification of a mixture containing unknown NOx adducts. The absence of a peak following injection of a sample into triiodide indicates the sample has no NOx adducts other than perhaps nitrate, the only NOx adduct not detected by triiodide. If the sample yields a signal in triiodide it can be attributed to the presence of nitrite, GSNO, DNICs and/or heme-NO. The presence of nitrosothiols can be derived from the difference between the signal observed in triiodide and that observed from a simultaneous or sequential injection of the sample into Ac/FeCN, which detects nitrite and iron nitrosyls but not nitrosothiols– if the sample is 100% nitrosothiols then no signal will be observed as illustrated. The Ac/FeCN signal, if present, will most likely be from either nitrite or FeNOs (heme or non-heme). Further injection of the sample into PBS/FeCN will provide a signal

that can only be ascribed to iron nitrosyl species. If no signal is observed in PBS/FeCN following a signal in Ac/FeCN then the signal was wholly from nitrite as illustrated. The amount of nitrite in a sample can be derived as the difference between the signals obtained following injection in to Ac/FeCN and PBS/FeCN. Alternatively, nitrite can be quantified by injection into Ac/Asc which yields a sharp peak only from nitrite. Any signal observed in PBS/FeCN could be due to either heme-NO or non-heme-NO such as DNICs. The presence of heme-NO can be selectively determined by injection of the sample into Ac/Asc, where it produces a peak that has slower kinetics and therefore is qualitatively different from that of nitrite. DNICs do not yield any significant peak in Ac/Asc.

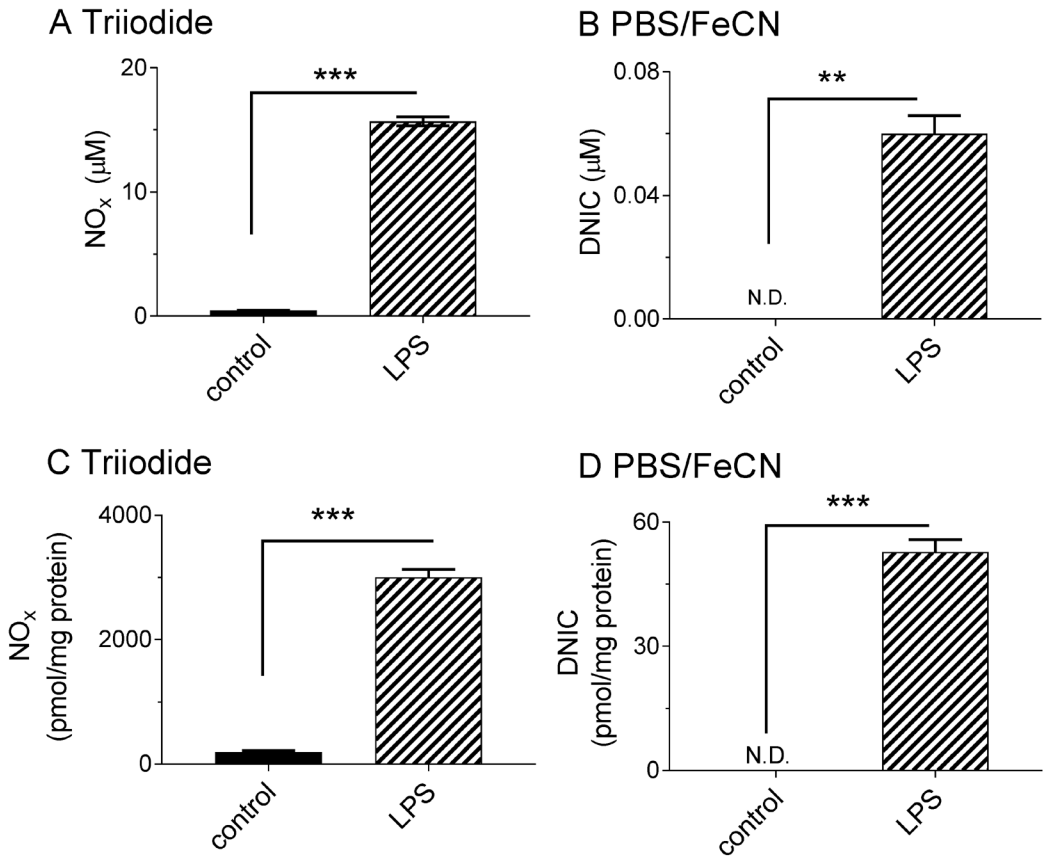

Figure 4.

NOx responses in RAW 264.7 macrophages treated with LPS. Cells were cultured in DMEM media with or without LPS for ten hours, after which NO_x was measured in the cell media (A, B) and in the cell lysates (C, D) with triiodide and PBS/FeCN. Note the 30-fold increase in cell media NOx as measured by triiodide demonstrating successful iNOS stimulation. Data are presented as mean ± SEM, $n = 3$, *= $p < 0.05$, **= $p < 0.01$, *** = $p < 0.001$.

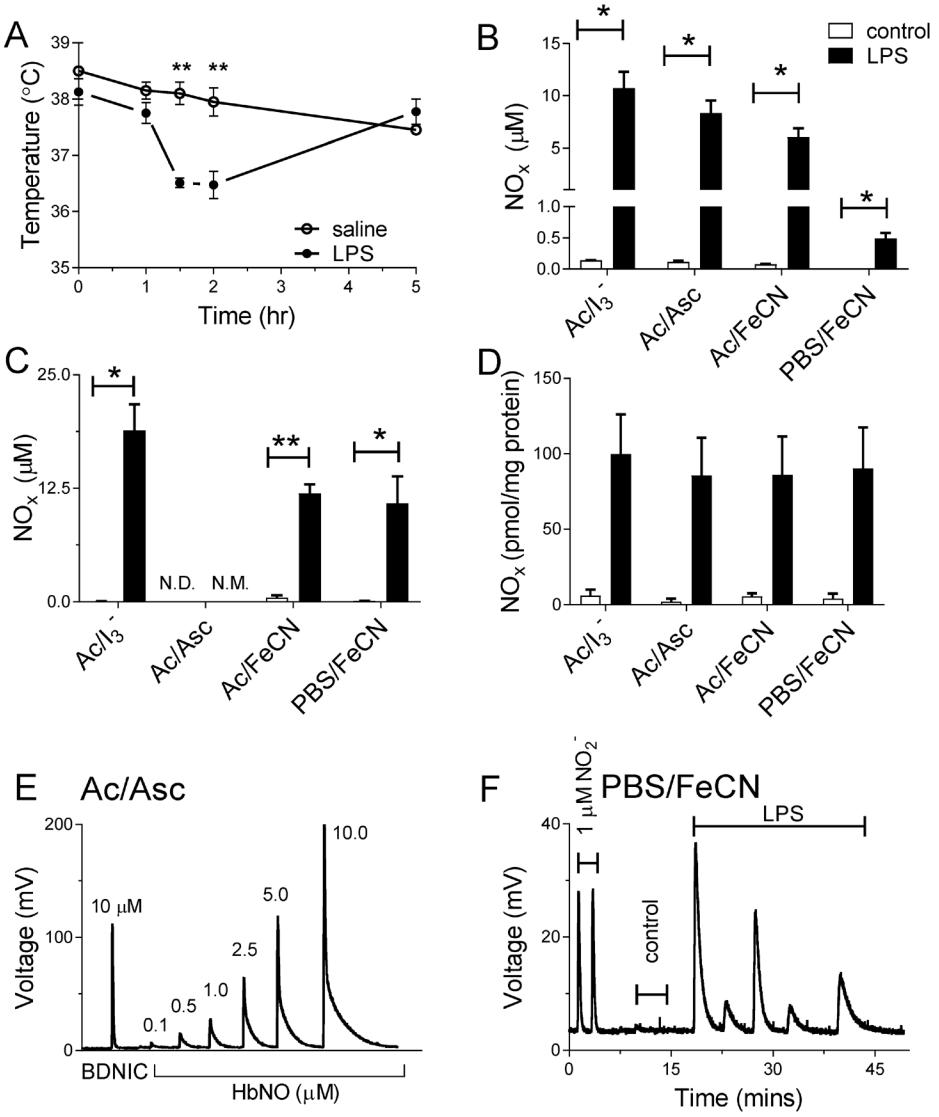

Figure 5.

A) Fall in rectal temperature of LPS-treated rats, demonstrating successful infection. B) Marked increases in NO_x in plasma and (C) whole blood of LPS-treated rats as determined by the various purge vessel reagents. D) Effect of LPS treatment on NO_x levels in liver homogenates as determined by different purge vessel reagents. E) Demonstration of how the Ac/Asc assay quantitatively releases NO from heme-NO (0.1 to 10 mM HbNO) but not DNICs. The small peak observed for DNICs is < 10% of the signal produced from an equivalent concentration of DNICs in triiodide and is scavengable by acidified sulfanilamide. The heme-NO peak in the Ac/Asc assay is qualitatively different from nitrite due to slower NO-release. F) NOx signal from the liver tissue homogenates in the Ac/Asc assay following detection of a signal in the PBS/FeCN assay. Since the Ac/Asc assay is not expected to detect DNIC, the NOx signal from the liver tissue homogenates in Ac/Asc is qualitatively similar to that of the heme-NO than nitrite, and the NOx levels in Ac/Asc are similar to the NOx levels measured by PBS/FeCN, most of the NO released from liver tissue

in the FeNO assay is more likely from heme-NO as opposed to DNICs. N.D. = not detected, N.M. = not measurable.

Table 1.

Applicability of different purge vessel reagents for releasing NO (g) from glut-B/MDNICs, nitrite and GSNO.

		NO_x Species		
Purge Vessel Reagent	**NO(g)**	**NO_2^-**	**RSNO**	**B/MDNIC**
Triiodide (Ac/I_3^-)	✓	✓	✓	✓
Ascorbic Acid in Acetic Acid (Ac/Asc)	✓	✓	ND	ND
Cu(ll) + Ascorbic Acid in Acetic Acid (Ac/Asc)	✓	✓	✓	ND
FeCN in Acetic Acid (Ac/FeCN)	✓	✓	ND	✓
FeCN in pH = 7.4 PBS (PBS/FeCN)	✓	ND	ND	✓

Tick mark = NO release; ND = not detected.